Nucl. Fusion **50** (2010) 035003 (8pp) doi:10.1088/0029-5515/50/3/035003

The super X divertor (SXD) and a compact fusion neutron source (CFNS)

M. Kotschenreuther[1], P. Valanju[1], S. Mahajan[1], L.J. Zheng[1], L.D. Pearlstein[2], R.H. Bulmer[2], J. Canik[3] and R. Maingi[3]

[1] Institute for Fusion Studies, The University of Texas at Austin, TX 78712, USA
[2] Lawrence Livermore National Laboratory, CA 94550, USA
[3] Oak Ridge National Laboratory, TN 37821, USA

E-mail: pvalanju@mail.utexas.edu

Received 12 January 2009, accepted for publication 14 January 2010
Published 12 February 2010
Online at stacks.iop.org/NF/50/035003

Abstract
A new magnetic geometry, the super X divertor (SXD), is invented to solve severe heat exhaust problems in high power density fusion plasmas. SXD divertor plates are moved to the largest major radii inside the TF coils, increasing the wetted area by 2–3 and the line length by 2–5. Two-dimensional fluid simulations with SOLPS (Schneider *et al* 2006 SOLPS 2-D edge calculation code *Contrib. Plasma Phys.* **46**) show a several-fold decrease in divertor heat flux and plasma temperature at the plate. A small high power density tokamak using SXD is proposed, for either (1) useful fusion applications using conservative physics, such as a component test facility (CTF) or fission–fusion hybrid, or (2) to develop more advanced physics modes for a pure fusion reactor in an integrated fusion environment.

PACS numbers: 52.55.Fa, 52.55.Rk

(Some figures in this article are in colour only in the electronic version)

1. Introduction

A steady-state fusion reactor will have much higher heating power P_h and pulse length than ITER [2], which itself is several times beyond current fusion machines. Invoking the standard measure P_h/R for the severity of the heat flux, we observe the following: (a) the two largest current tokamaks JET and JT-60 each have $P_h/R \sim 7$, (b) ITER, with $P_h \sim 120$ MW and $R \sim 6.2$ m, has $P_h/R \sim 20$, but (c) even a moderate fusion reactor [3–6] ($P_h \sim 400$–720 MW at $R \sim 5$–7 m) will have a much larger $P_h/R \sim 80$–100 and (d) larger values yet obtain for proposed spherical tokamak reactors [7, 8]. Even for more modest power fusion devices such as component test facilities (CTF) [9–11] or a compact fusion neutron source (CFNS) for a fission–fusion hybrid [12, 13], the P_h/R will be substantially larger than ITER's P_h/R. Also, for such small devices, the length along a field line from the outboard plasma to the divertor plate will be much less than for ITER. ITER-like standard divertors (SDs) cannot be expected to handle such large increases in heating power density [14] and reductions in line length.

The 2007 ITER Physics Basis identifies divertor limitations as a key roadblock to higher fusion power densities in steady-state scenarios [15]—'The fusion gain in steady state maximizes at low density for constant β_N. The limitation on reducing the density in next generation tokamaks is set by the impact on the divertor'. The super X divertor (SXD) was developed precisely to meet the challenge of high power density simultaneously with lower plasma density.

This high power density, coupled with the range of scrape-off layer (SOL) projections, implies that an acceptable divertor operation is, perhaps, the most serious roadblock in the march towards achieving economically desirable power densities for fusion. A high SOL power density leads to operation in the sheath-limited regime—an unacceptable regime associated with high plate erosion, low impurity shielding, low neutral pressures making helium exhaust problematic or virtually impossible, and low divertor radiation and high divertor heat fluxes. Attempts to dissipate excess heat via core radiation preclude good confinement, and probably high β [14]. The low power density of ITER gives a P_h/R sufficiently low to allow a SD to cope, but such SDs are not likely to extrapolate to power densities several times higher. While a much higher divertor plate tilt might ameliorate the heat flux difficulty, it does not significantly improve other problems of operation in the sheath-limited regime.

The SXD [16], created via a redesign of the divertor magnetic geometry, appears to offer a simple and robust, axisymmetric solution for high power density divertor operations. By maximizing divertor power capacity, SXD

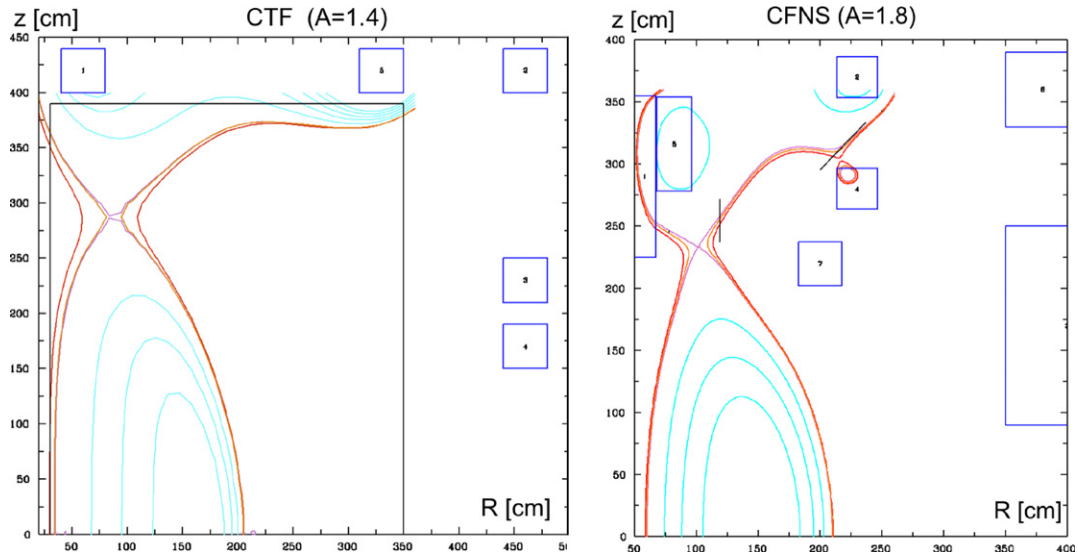

Figure 1. CORSICA SXD equilibria: left—for low-A CTF with only one extra SXD coil; right—for CFNS.

reduces the core radiation burden, and thus enables core plasma operation to attain high density of fusion power production. As we will see, unique features of the SXD geometry give it substantial advantages over other flux expansion schemes.

Simulations using SOLPS [17–21] for SXD equilibria generated with CORSICA [22] show striking SXD advantages. In this paper, we consider specific parameters for a tokamak, and quantitatively display the advantages of the SXD via simulation and analysis. We choose parameters for a low aspect ratio tokamak with small size but high power density—100 MW fusion power with a major radius of 1.35 m. It could potentially be used for many missions: (1) a fusion CTF, (2) a CFNS for a fission–fusion hybrid or (3) as an inexpensive test bed to experimentally demonstrate the compatibility of advanced plasma core operation with a much more challenging divertor environment than ITER, as a prelude to an advanced fusion power plant. The divertor of such a device is very challenging—the SOL particle density is comparable to ITER and pure fusion power plants, the upstream parallel heat flux is somewhat higher than ITER, but because of its small size, the connection length is many times less than ITER. For a SD, this would lead to operation well into the sheath-limited regime. However, we find that the SXD robustly avoids this regime, as we believe is required of any practical application of tokamak-based fusion.

2. SXD: magnetic design

The SXD is an improvement upon the X-divertor (XD) [14]. In the XD, flux expansion near the divertor plate was significantly increased by producing an additional X-point near where the separatrix meets the divertor plate. The SXD improves upon this by additionally increasing the major radius of the divertor. This can be done while keeping the main plasma geometry essentially unchanged. Typically, SXD configuration can increase the major radius by a factor of 2–3, and so it is superior to the XD by increasing the wetted area by factors of 2–3, and also similarly increasing the line length. The SXD has the same relative advantage compared with other proposed geometries (placing the divertor plate near the main X-point, extreme plate tilting, snowflake divertor [23], etc). Compared with previous proposals, the SXD maximizes several advantageous features at once.

To gain insight into the gross effects of geometry alone on the heat flux, we derive a simple analytical expression with the simplifying assumptions that the power which makes it into the upstream SOL follows the field lines to the divertor plate, and we neglect losses from atomic physics. Then the plasma-wetted area A_w on the divertor plates is approximately

$$A_w = \frac{B_{p,sol}}{B_{div}} \frac{A_{sol}}{\sin(\theta)} \approx \left[\frac{B_p}{B_t}\right]_{sol} \frac{R_{div}}{R_{sol}} \frac{A_{sol}}{\sin(\theta)}$$
$$= \left[\frac{B_p}{B_t}\right]_{sol} \frac{2\pi R_{div} W_{sol}}{\sin(\theta)}, \quad (1)$$

where R_{sol}, W_{sol} and A_{sol} are the radius, width and area of the SOL at the midplane, θ is the angle between the divertor plate and the total magnetic field B_{div}, and the subscripts p and t denote the poloidal and toroidal directions, respectively. For a plasma with a given W_{sol} and B_p/B_t at midplane SOL, A_w can be increased only by reducing θ or by increasing divertor plate major radius R_{div}. Due to engineering constraints, θ must be greater than about 1°, so the only remaining 'knob' to increase A_w is to increase R_{div}. SXD does just this with axisymmetric PF coils.

The surprising discovery is that a large increase in R_{div} can be achieved with relatively small modifications (in positions and currents) to the conventional poloidal field (PF) coils for a SD of a large range of devices. *For all these devices the TF coils of the original design were retained in their entirety; therefore, the volume inside the TF coils was not increased.* In figures 1 and 2, we show SXD CORSICA equilibria for a low aspect ratio CTF [9], a low aspect ratio CFNS for a fission–fusion hybrid [12, 13], for FDF [11] (a proposed CTF with $A = 3.4$), and for the superconducting (SC) SLIM-CS reactor [4]. The SLIM-CS case shows that an SXD can be obtained with SC coils all outside the TF coils.

The SXD can also be designed for a wide variety of plasma shapes and parameters, using all axisymmetric PF coils, or

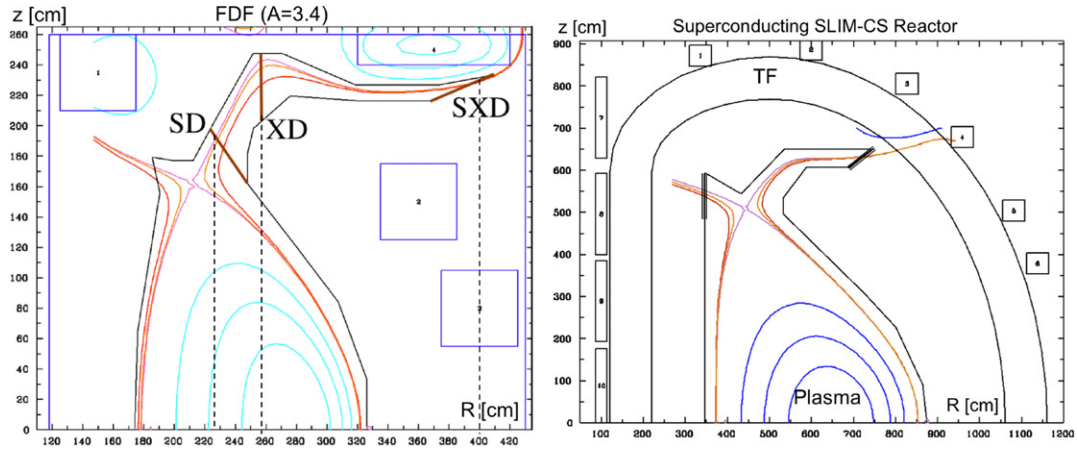

Figure 2. Left: SXD for FDF; right: SLIM-CS reactor with SC PF coils outside TF.

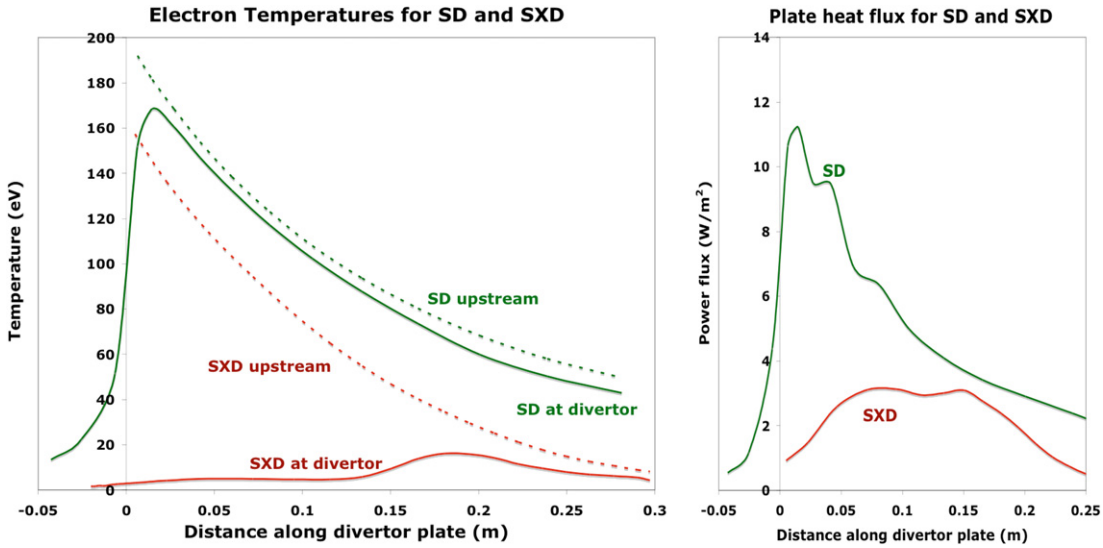

Figure 3. Left: electron temperatures for the SD and SXD along the divertor plate. Upstream temperatures are mapped along a flux surface to their position on the divertor plate. Upstream density is 2.9×10^{19} for both cases Right: heat flux along the divertor plate for the SD and SXD.

with modular PF coils as in [14]. The change in the total PF coil Amp-meters for SXD is usually only about $\pm 5\%$ from the SD case.

In general, the best way to deploy SXD is in a double-null configuration where the large majority of the power exhaust goes to the outer divertor legs. With even a fivefold reduction in peak heat flux on the outer SXD legs, the inner legs do not become the limiting factor.

The SXD geometry for the CFNS is analysed in more detail in the following. For the geometry considered, the parallel field line length is increased from 6 m for the SD to 13 m for the SXD. The divertor plate is at a radius which is about 1.9 times larger in the SXD case, with a commensurate reduction in the magnetic field at the divertor plate.

3. SXD: simulations of the CFNS with 2D fluid codes

Simulations of the CFNS geometry have been performed using SOLPS. The perpendicular transport coefficients are chosen to be spatially uniform and have the same values as are conventionally used in simulations of ITER (e.g. the perpendicular heat diffusivity is $1\,\mathrm{m^2\,s^{-1}}$). Parallel flux limits are used so that the parallel heat flux remains below the maximum possible for a one-sided Maxwellian. The SOL power is taken to be 50 MW in these cases, which is realistic for the anticipated CFNS operation.

To ameliorate the high heat fluxes found in the SD, the divertor plate is much more highly tilted than in the case of ITER. The tilt angle between the total magnetic field and the plate is taken to be 1°, which is about the minimum value thought possible for ITER due to engineering considerations. For a consistent comparison, the SXD has the same tilt angle.

Figure 3 shows SOLPS results for the CFNS (no impurities) in figure 1. We compare an SD case and an SXD case with the same SOL density at the outboard midplane separatrix ($2.9 \times 10^{19}\,\mathrm{m^{-3}}$—a typical value expected for CFNS operation as explained below). The SD case is in the sheath-limited regime—the divertor electron temperatures are nearly the same as the upstream plasma temperatures at the outboard midplane, when the upstream temperatures are mapped to the same flux surface as the divertor positions. This is not surprising, since the upstream plasma density is about the same as ITER, the

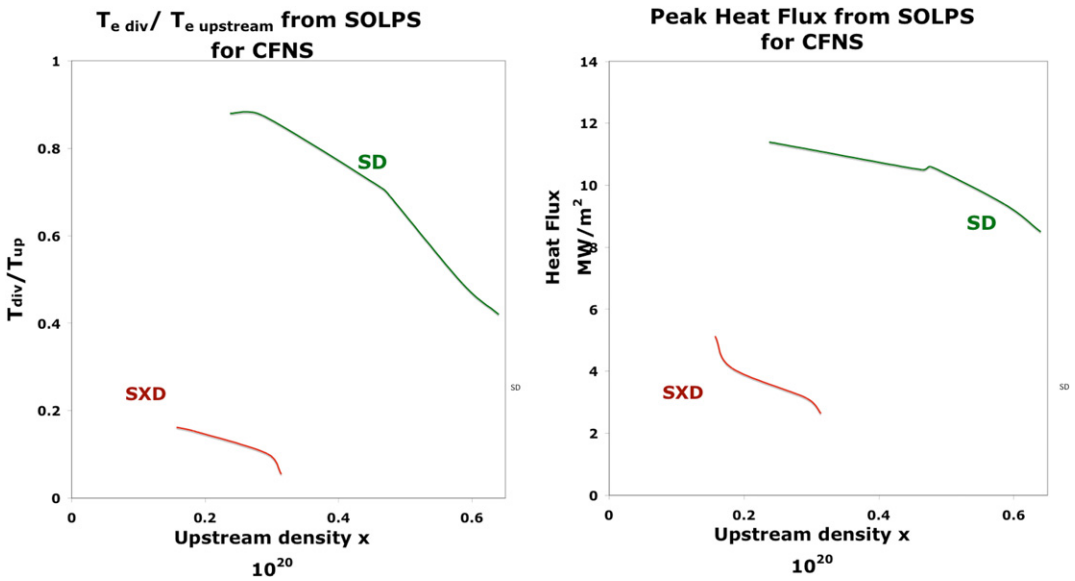

Figure 4. Left: ratio of the peak divertor electron temperature at the divertor to the peak upstream temperature versus upstream density for the SD and SXD. The SXD avoids the sheath-limited regime for much lower upstream density. Right: peak heat flux for the SD and SXD versus upstream density. All cases have $P_{\mathrm{SOL}} = 50$ MW going into the SOL.

upstream parallel heat flux is about 1.5 times ITER, and the line length is almost an order of magnitude less than ITER.

The SXD has much lower heat flux and plasma temperature at the divertor plate than in SD. With the SXD, the divertor plasma temperatures are overall about an order of magnitude lower than the upstream temperatures. Near the separatrix, the plasma temperature at the divertor plate is only 2–3 eV, and the pressure at the divertor plate is reduced by a factor of 4 from the upstream values. Hence, the SXD divertor plasma is in the partially detached regime.

Figure 4 displays the variation of the ratio of the peak divertor electron temperature to the peak upstream SOL electron temperature, and peak heat flux with upstream density. The SXD avoids the sheath-limited regime for densities which are much lower than is the case for the SD. This has very important implications for the practicality of current drive in steady-state devices such as the CFNS, as we describe later.

With an SD, the strong plate tilting has reduced the heat flux to a value only slightly higher than desired in ITER. However, the extremely high plate temperature leads to equally debilitating problems such as plate sputtering and erosion, low impurity screening and likely very low helium exhaust. Quantitative analysis of these problems will be performed in future investigations.

4. The SXD: semi-analytical results using simplified models

The SOLPS simulations find that the SXDs can reduce T_{div} from 100–200 eV to ~10 eV. Of course, this is highly significant, and so we have performed analytical investigations to understand this. These results find that the SXD geometry alone, together with conventional parallel physics and sheath physics, leads to a large reduction in the plasma temperature near the divertor plate. Of course, when the divertor plate temperature is low (and divertor density is high), physical processes become operative to reduce the heat flux and temperature even more than would be expected from geometry alone (such physical effects include atomic effects such as charge exchange and ionization, radiation and also potentially perpendicular transport near the plate). The crucial requirement is to reduce the plate temperature to a range where these physical processes become strong. The simplified semi-analytical models considered here are very helpful in understanding why the temperature can be reduced from very high values to much lower values where additional physical processes, outside these models, can operate strongly.

These models find that the much lower value of *total* B field at the divertor plate (due to the larger major radius) can be identified as the dominant causative factor for the reduction in temperature: as a flux tube goes from a region of high B to low B, its cross sectional area increases. Since the power flow through an SOL flux tube is nearly constant (neglecting cross-field transport and atomic effects), the parallel heat flux $Q_{\parallel}$ is reduced as the area is increased. Since the sheath temperature is determined by $Q_{\parallel}$ (but is virtually independent of the plate tilt or poloidal flux expansion), the sheath temperature decreases strongly as the divertor plate is moved towards the lower total B (larger R) region. It is found that this has a much stronger effect on the plasma temperature than the increase in line length. This physical effect is unique to the SXD geometry, since it results from the placement of the divertor plate at much larger major radius and hence lower total B. Other geometries (such as the X-divertor, the snowflake divertor or much stronger plate tilting) do not have the purely geometrical reduction in the parallel heat flux near the divertor plate that results from the SXD geometry.

The simplest divertor model is the 'two-point model' [24] (which assumes Spitzer electron heat conduction, pressure balance along a field line and a sheath boundary condition). The effect of B variations can be straightforwardly included, with the assumption that the magnetic field is reduced only near the divertor plate. The results are shown in figure 5. For

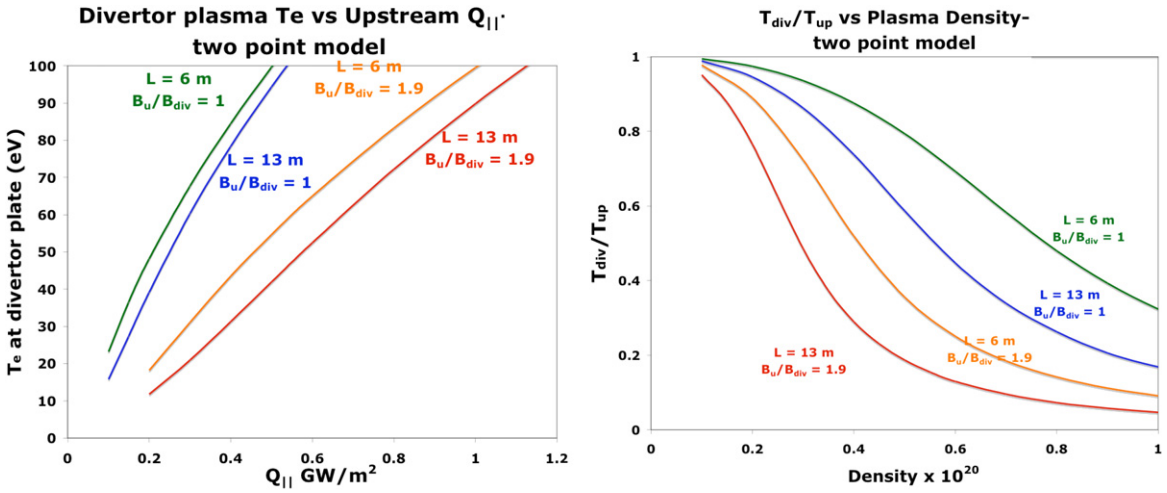

Figure 5. Left: divertor electron temperature versus parallel heat flux for an upstream density of 3×10^{19}. Right: ratio of divertor temperature to upstream temperature for a parallel heat flux of 0.5 GW m^{-2}.

parameters typical of a CFNS with an SXD, the reduction in $T_{\rm div}$ is primarily due to reduced B at the plate; the increased line length typical of the SXD is less significant. The SXD gives a low plate temperature for much higher values of the upstream $Q_\parallel$—by a factor of about 3. Alternatively, the model shows that the SXD geometry avoids the sheath-limited regime for much lower densities than the SD—by a factor of about 3. We have also numerically solved a more complete 1D model of SOL physics. Coupled differential equations describe separate electron and ion parallel transport (Spitzer conduction plus flux limits), classical electron–ion equilibration, pressure balance of the total pressure and conventional sheath physics (details of the model are in the appendix). As shown in figure 6, the relative advantage of the SXD is about the same with this more complete physics model: the SXD allows about a factor of 3 higher upstream $Q_\parallel$ while maintaining a low plate temperature, and the sheath-limited regime is reached for a density which is about 3 times lower than for the SD.

A simple criterion, from the two-point model, to determine whether the divertor is in the sheath-limited regime, reads as $S = Q_{\parallel u}(B_{\rm div}/B_{\rm up})^{1.75}/n^{1.75}L^{0.75} > 1 \times 10^{-27}$ W/m$^{2.5}$ in MKS units. The original analysis [24] did not include the possibility of significant variations in B in the SOL. We find it can be included through the factor $(B_{\rm div}/B_{\rm up})^{1.75}$, where up and div refer to quantities evaluated at the location of the outboard midplane upstream and divertor, respectively.

In conclusion, both the two-point model and the more complete 1D model imply that the advantages of the SXD result less from the increased line length and more from the geometrical reduction in the parallel heat flux due to the expansion of a flux tube as it travels into a region with a lower total magnetic field.

5. Additional divertor considerations

Transient heat fluxes from ELMS and disruptions are also an issue for the divertor plates. To the extent that such heat pulses follow field lines, the SXD is expected to spread them over a larger wetted area, and also possibly a longer time (the longer line length would lead to longer parallel pulse propagation times), compared with an SD. These effects would reduce the divertor plate erosion. However, effects from cross-field heat fluxes on the long divertor throat need further consideration that is beyond our scope here.

Some ELM mitigations will likely be required for the CFNS. The ratio of the pedestal stored energy to the wetted area on the divertor is about 2.6 MJ m^{-2} for the CFNS with an SXD, whereas the same ratio for ITER is about 19 MJ m^{-2}. The ELM energy deposition in the CFNS could be more rapid than in ITER because the connection length is about 4 times smaller for the CFNS (with an SXD). Recall that the metric for tolerable ELM size scales as MJ m^{-2} s$^{-1/2}$. Let us presume that the same fraction of pedestal energy is lost per ELM in ITER as in the CFNS. Then in the CFNS, the ELMs are about 3–4 times 'smaller' in the appropriate metric. Hence, some ELM mitigation may be required for the CFNS, but probably considerably less so than for ITER.

Unlike SD, SXD plates are far enough from the plasma so that substantial neutron shielding could be provided. Preliminary neutron transport calculations with MCNPX find that shielding reduces neutron damage by several times—which might allow a CFNS or a DEMO to employ more near-term divertor materials (e.g. Cu or CFCs) that would otherwise undergo severe degradation. Detailed neutronic calculations will be presented elsewhere.

Other potential benefits of the SXD geometry are worth noting. By placing the plates much further from the plasma, the SXD geometry may reduce the effects of halo currents on the complex divertor components. It can enable operation at much lower core radiation and edge density—thus reducing disruption probability. The SXD is also fully compatible, and sometimes synergistic, with other methods such as using liquid metals (since MHD drag is lower at small B, and the long divertor throat shields evaporated impurities).

6. A CFNS using the SXD

The mission of a compact fusion device (CFNS) using the SXD could be either (1) short term fusion applications using

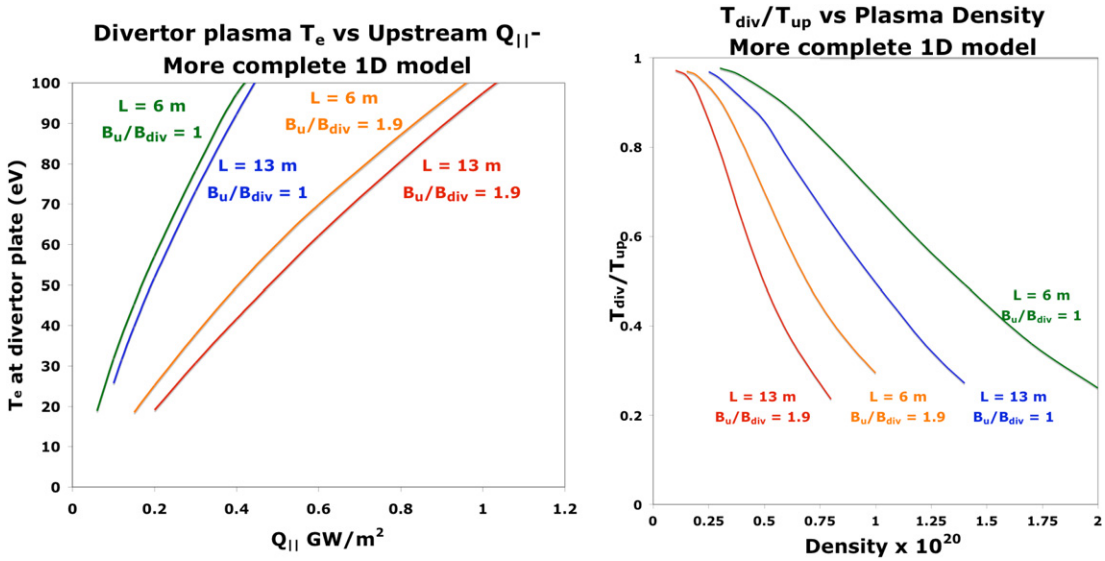

Figure 6. Left: divertor electron temperature versus parallel heat flux for an upstream density of 3×10^{19}. Right: ratio of divertor temperature to upstream temperature for a parallel heat flux of 1.0 GW m^{-2}.

conservative physics, such as a CTF or a fission–fusion hybrid, or (2) to provide a test bed to develop advanced physics modes for a pure fusion reactor in an integrated fusion environment with high heat fluxes.

To quantitatively demonstrate the importance of SXD for a CFNS, we choose a compact reference device with a set of reasonable but definite parameters. For low size, coil mass and easy maintenance, we consider a low aspect ratio (A), Cu coil device. We take $A = 1.8$, $R = 1.35$ and elongation $\kappa = 3$. A fusion power of 100 MW gives to the CFNS a neutron wall load of ∼1 MW m^{-2}. We take the B field at the centre post as 7 T, less than or equal to the value in ST reactor [7, 8] and CTF studies [9, 10].

We consider the physics requirements of a CFNS, by computing the dimensionless physics parameters $\langle\beta\rangle_N$ and H. (Here $\langle\beta\rangle_N = (\langle p\rangle/\langle B^2\rangle)/(I/aB)$ and $\langle B^2\rangle$ is the volume averaged *total* B^2. The no-wall stability limit is $\beta_N \sim 3$ for all aspect ratios for this $\langle\beta\rangle_N$ [25].) H is the confinement enhancement above ITER98H(y, 2).

There is significant evidence that low aspect ratio devices have a more optimistic scaling with collisionality ν_* than ITER98H(y,2) [26]. To account for this possibility, we consider, in addition to the standard H factor, a modified H factor, $H' \sim H\nu_*^{-\alpha}$. H' is normalized so that the MAST range of ν_* as $H' \sim 1$. Preliminary experimental results indicate $\alpha \sim 0.2$. In the conservative case below, we choose a more conservative enhancement factor of $\alpha = 0.1$. In the advanced case, we take $\alpha = 0.2$.

To calculate the current drive power for a 100 MW fusion power at a given $\langle\beta\rangle_N$, we use an estimated current drive efficiency $In_eR/P_h = 0.15 \times 10^{20}(\langle T_e\rangle/10\,\text{kev})\,\text{A W}^{-1}\,\text{m}^{-2}$. This is somewhat more conservative than what is found in reactor studies and ITER analysis, since the higher trapped particle fraction at a low aspect ratio makes current drive more difficult. Numerical VMEC [27] equilibria, with fixed temperature and density profile shapes—characteristic of low collisionality hybrid H-modes—are used to determine $\langle\beta\rangle_N$, the bootstrap current and the fusion power from thermal cross sections. The total current is the sum of bootstrap and driven currents.

To connect the core analysis with the SOLPS simulations, we estimate that the SOL density is 1/4 of the core density, similar to experimental results on NSTX. We presume core radiation reduces the heating power that falls into the SOL to 50 MW. When evaluating the H factor requirement, this core radiation power is subtracted from the heating power [14].

We consider two scenarios. One is for a relatively conservative core operation for near-term applications, such as a CTF or a CFNS for a fission–fusion hybrid. The scenario has $Q < 3$ and $\langle\beta\rangle_N = 2.5$, to stay significantly below the no-wall limit and attain a low potential for disruptions. The bootstrap fraction is ∼30–40%. In the second, we consider an advanced scenario with core parameters similar to those assumed in tokamak fusion reactor studies for advanced operation: $Q \sim$ 4–10, $\langle\beta\rangle_N = 4.3$ and bootstrap fractions ∼70–80%. This scenario is well beyond the operation anticipated on ITER, so some experimental demonstration would likely be required—to demonstrate reliable operation with a low chance of disruptions in a primarily self-heated plasma, with viable edge conditions—before an expensive DEMO based on such parameters would be built. As with reactors, high Q for this scenario in a CFNS requires sufficiently low density for adequate current drive efficiency.

We first consider the conservative case. Consistent with the ITER physics basis, we read from figure 7 that the current drive power requirement increases strongly with the density, resulting in low fusion gain and very high current drive power requirements at high densities. At lower densities, with better current drive efficiency, divertor operation becomes problematic with the SD. A comparison of the upstream and downstream values of the temperature and pressure from the simulations implies that the SD is well into the sheath-limited regime, whereas the SXD is in the high recycling or partially detached regime. The SXD allows operation in a regime with a relatively low current drive power, $Q \sim$ 1–3, and confinement requirements consistent with expectations for an H-mode. The

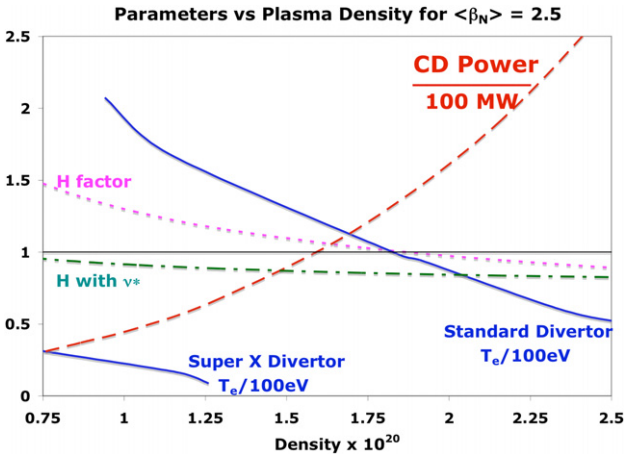

Figure 7. Left: parameters versus density for the compact 100 MW fusion device for $\langle\beta\rangle_N = 2.5$. Divertor temperatures are very high for the SD.

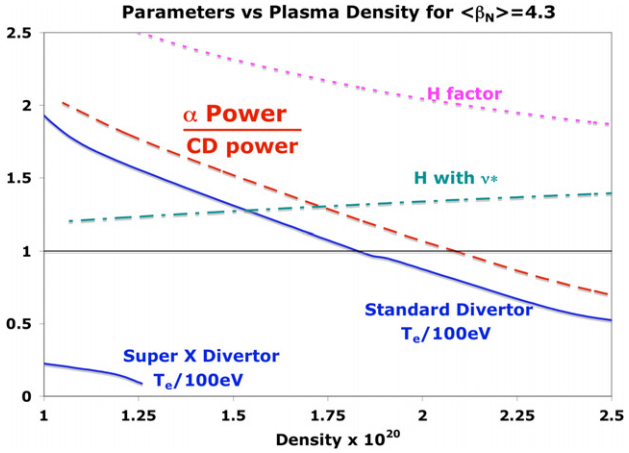

Figure 8. Parameters versus density for an advanced tokamak operation with 200 MW fusion power. The divertor plasma temperature is very high for the SD.

SD is in the sheath-limited regime, except at high densities which have extremely large current drive power requirements, >200 MW, and $Q \sim 1/2$. For such high external powers, large core radiation power (>150 MW) is needed to give satisfactory divertor operation for the SD. This would lead to sustained high peak surface heat flux on the main chamber first wall ($>1.5\,\mathrm{MW\,m^{-2}}$) which is a serious engineering feasibility issue with near-term structural materials. (Design studies of tokamak fusion reactors [3–8] limit the main chamber heat flux to values 0.5–1 $\mathrm{MW\,m^{-2}}$.)

The midrange densities of figure 7 are at about a third of the Greenwald limit. Together with low radiation fractions in the low density range, this should help to give a low disruption probability.

We now consider an advanced operation. The high $\langle\beta\rangle_N$ leads to a higher fusion power (200 MW), even with reduced driven currents (to attain higher bootstrap fractions). The SXD allows operation in a regime with high Q, so that the alpha power exceeds the heating power—to enable experiments on primarily self-heated plasmas pertinent to a reactor. As before, the SD is in the sheath-limited regime, except at high densities where the plasma is not primarily self-heated. As is always the case when projecting confinement for an advanced operation, the ability to attain the required high confinement is quite uncertain (figure 8).

7. Conclusion

By increasing R_{div}, the SXD geometry significantly reduces the heat flux and the plasma temperature at the divertor plate. Analytic arguments and SOLPS simulations show that the SXD can avoid the sheath-limited regime for much higher SOL powers, or lower SOL densities, than for conventional divertors. If verified by experiments, these benefits would allow much higher power density tokamaks to operate with a steady-state current drive. A CFNS using SXD could produce a neutron wall load $\sim$1 $\mathrm{MW\,m^{-2}}$ with conservative physics, but could also be capable of demonstrating high integrated physics performance in the advanced tokamak regime.

Acknowledgment

This research was supported in part by USDOE Contracts DE-FG02-04ER54742, DE-FG02-04ER54754 and DE-AC05-00OR22725.

Appendix

The equations used in the one-dimensional model include parallel heat conduction, pressure equilibration, classical electron–ion energy transfer and the sheath boundary condition. We neglect cross-field energy transport and atomic processes, so for each species, electron–ion equilibration is the only process which changes the total power along a flux tube. So for ions

$$\frac{\mathrm{d}}{\mathrm{d}l}A(l)\,Q_{\parallel \mathrm{i}} = \frac{n\,(T_\mathrm{e} - T_\mathrm{i})}{\tau}A(l), \qquad \text{(A1)}$$

and the corresponding equation for electrons is obtained by interchanging subscripts e and i. Here, $A(l)$ is the flux tube cross section as a function of position along the flux tube l. For each species, we use the classical expression for the parallel heat flux, and roughly include kinetic effects by adding heat flux limits:

$$\frac{1}{Q_{\parallel \mathrm{i}}} = \frac{1}{Q_{\parallel \mathrm{iclass}}} + \frac{1}{K n v_{\mathrm{thi}} T_\mathrm{i}}, \qquad \text{(A2)}$$

where $Q_{\parallel \mathrm{iclass}}$ is the classical collisional heat flux $\kappa_\mathrm{i}\mathrm{d}T_\mathrm{i}/\mathrm{d}l$, and the flux limit coefficient K is taken to be 1.5, in the range indicated by a recent review [28]. The sheath boundary conditions are taken from a recent review [24].

References

[1] Schneider R. *et al* 2006 SOLPS 2-D edge calculation code *Contrib. Plasma Phys.* **46** 3–191
[2] Shimada M. *et al* 2007 *Nucl. Fusion* **47** S1-17
[3] Najmabadi F. *et al* 2006 *Fusion Eng. Des.* **80** 3
[4] Sato M. *et al* 2006 *Fusion Eng. Des.* **81** 1277
[5] Okano K. *et al* 2006 *Nucl. Fusion* **40** 635
[6] Cook I., Taylor N. and Ward D. 2003 *Proc. Symp. on Fusion Engineering (San Diego, CA, USA, 2003)* p 39 http://ieeexplore.ieee.org/xpl/tocresult.jsp?isnumber=11108&isYear=1995

[7] Voss G.M., Bond A., Hicks J.B. and Wilson H.R. 2002 *Fusion Eng. Des.* **63–65** 65
[8] Najmabadi F. *et al* 2003 *Fusion Eng. Des.* **65** 141
[9] Peng Y.-K.M. *et al* 2005 *Plasma Phys. Control. Fusion* **47** B263
[10] Voss G.M. *et al* 2008 *Fusion Eng. Des.* **83** 1648
[11] Stambaugh R.D. *et al* 2007 *Bull. Am. Phys. Soc.* **52** NP8.00123
[12] Peng Y-K M. *et al* 1995 *16th IEEE/NPSS Symp. on Fusion Engineering (Champaign, IL, USA)* p 1423 http://ieeexplore.ieee.org/xpl/tocresult.jsp?isnumber=11108&isYear=1995
[13] Kotschenreuther M. *et al* 2009 *Fusion Eng. Des.* **84** 83
[14] Kotschenreuther M., Valanju P. and Mahajan S. 2007 *Phys. Plasmas* **14** 072502
[15] Gormezano C. *et al* 2007 *Nucl. Fusion* **47** S285
[16] Valanju P., Kotschenreuther M. and Mahajan S. 2009 *Phys. Plasmas* **16** 056110
[17] Schneider R. *et al* 1992 *J. Nucl. Mater.* **196–198** 810
[18] Reiter D. 1992 *J. Nucl. Mater.* **196–198** 80
[19] Coster D. *et al* 2000 *Proc. 18th Int. Conf. on Fusion Energy 2000 (Sorrento, Italy, 2000)* (Vienna: IAEA) CD-ROM file EXP5/32 and http://www.iaea.org/programmes/ripc/physics/fec2000/html/node 1.htm
[20] Coster D. *et al* 2002 *Proc. 18th Int. Conf. on Fusion Energy (Lyon, France, 2002)* (Vienna: IAEA) CD-ROM file TH/P2-13 and http://www.iaea.org/programmes/ripc/physics/fec2002/html/fec2002.htm
[21] Coster D. *et al* 2004 *Phys. Scr.* T **108** 7
[22] Crotinger J.A., LoDestro L.L., Pearlstein L.D., Tarditi A., Casper T.A. and Hooper E.B. 1997 *LLNL Report* UCRL-ID-126284, available from NTIS PB2005-102154
[23] Ryutov D. 2007 *Phys. Plasmas* **14** 06452
[24] Stangeby P.C. 2000 *The Plasma Boundary of Magnetic Fusion Devices* (London: Taylor and Francis)
[25] Friedberg J.P. 2007 *Plasma Physics and Fusion Energy* (Cambridge: Cambridge University Press)
[26] Valovic M. *et al* 2005 *Nucl. Fusion* **45** 942
[27] Hirshman S.P. and Whitson J.C. 1983 *Phys. Fluids* **26** 3553
[28] Fundamenski W. 2005 *Plasma Phys. Control. Fusion* **47** R163